ICAS 2021 SHANG HAI
International Council of the Aeronautical Sciences
32nd Congress of the International Council of the Aeronautical Sciences
September 6-10, 2021 Pudong Shangri-La, Shanghai, China

SIMULATION OF HIGH REYNOLDS NUMBER VISCOUS FLOW BASED ON ADAPTIVE CARTESIAN GRID

CHEN Hao[1,2], YUAN Xianxu[1,2],MENG Shuang[1,3], HUA Ruhao[2], TANG Zhigong[2], BI Lin[1,2 *]

[1]State Key Laboratory of Aerodynamics, China Aerodynamics Research and Development Center, Mianyang, 621000, China 1

[2]Computational Aerodynamics Institute, China Aerodynamics Research and Development Center, Mianyang, 621000, China 2

[3]Key Laboratory of Traffic Safety on Track, Central South University, Changsha 410075, China 3

Abstract

An adaptive Cartesian grid methodology approach is presented to compute two-dimensional high Reynolds number viscous flows. In this methodology, the immersed boundary approach is developed to deal with the boundary condition, which performs good ability in the simulation of viscous flows. An Octree data structure is used for grid information storage, making it convenient to accomplish grid adaptation. The Cartesian mesh is optimized by the mesh smoothing technology and the virtual layer method with the advantage of the body-fitted structured mesh. The virtual layers are formed in an increasing distance from the wall with the aim to obtain a desired ratio between neighboring cells, making sure the cell size changes gradually. Aiming at overcoming the difficulty of simulating high Reynolds number viscous flow based on Cartesian grid, a wall function method combined with immersed boundary method is also introduced. The numerical results prove that it can significantly reduce the dependence of numerical results on grid scale, which reduces the quantity of grids and enhances the computation efficiency dramatically. Meanwhile, a viscous numerical solver applicable to the adaptive Cartesian grid is constructed in this paper thanks to an appropriate discretization procedure. In this study, the methodology and numerical solver above are demonstrated with several typical cases.

Keywords: Adaptive Cartesian grid; immersed boundary method; wall function method

1. General Introduction

With the deep application of computational fluid dynamics (CFD) in engineering practice, the geometric shape and flow field are becoming more and more complex, and the generation of high-quality meshes is becoming more and more difficult, which often takes up a lot of human resources. Compared with the traditional structured mesh generation method and unstructured mesh generation method [1-3], the adaptive Cartesian mesh [4-6] has great advantages in automatically generating high-quality mesh for complex shapes. In addition, the adaptive Cartesian grid also has the natural multigrid characteristics, which can accelerate the convergence in the calculation. it does not need to store matrices, and has less operation, which is conducive to the application of high-precision algorithms. Since the 1980s, the rapid development of computer technology and performance has promoted the appli-cation and popularization of adaptive Cartesian grid technology. In view of the above advantages, more and more CFD workers have devoted themselves to the research and application of this method.

The main disadvantage of adaptive Cartesian mesh generation technology is that the boundary treatment of viscous surface is complex, which is caused by the non-body-fitted characteristics of Cartesian mesh. Cartesian grids generally intersect with the surface of the object to produce cutting elements of different shapes. Some of these cutting elements are small in size, which can easily cause the non-physical oscillation of the solution near the sur-face. If the difference scheme used in the numerical simulation is explicit, it will also limit the time step and affect the stability of the calculation. At present, the main processing methods are hybrid cell method [7,8], cut cell method [9,10], embedded boundary approach [11] and immersed boundary approach [12-13]. In these methods, the immersed boundary approach does not need to deal with the complex mesh-cutting problem. It is relatively simple and feasible. Moreover, the boundary layer characteristics

can be captured by ghost cell method with the help of adjustable reference points. In this paper, the method is used to construct the boundary conditions of viscous flows.

When the near-wall body-fitted grid extends outwards, the grid points are generally arranged in a certain pro-portion. The size of the grid increases gradually and the change is more uniform. This kind of grid characteristics is in good agreement with the boundary layer characteristics, which is conducive to capturing the flow characteristics of the boundary layer. However, for Cartesian grids, the distance of grid points in different sizes of adjacent grids is fixed, even in the boundary layer. This will affect the accuracy of numerical solution in the boundary layer and reduce the quality of the flow field simulation. Aiming at the problem of Cartesian grid, Ya'eer Kidron et al. [14] of Israel CFD Center first introduced the virtual layer method, which lays out some virtual surface layers near the object surface. The shape of the virtual surface layers are identical but the size are different, and the distance be-tween each layer is similar to the body-fitted structure grid. Along the direction perpendicular to the object surface, the number and level of Cartesian grids are determined by these virtual surface s. This method fully draws on the advantages of body-fitted grid. Ya'eer Kidron et al. combines it with the adaptive Cartesian grid method. At the same time, the cut cell method is used to deal with the surface, and good results have been achieved in the application. At present, there is no research on the combination of virtual layer method and immersed boundary method, which has space and value for further exploration and development. This is also one of the research contents to be carried out in this study.

Compared with the body-fitted grid, the Cartesian grid is non-body-fitted, and intersects with the object surface to form cutting grids with different size and shape. When Cartesian mesh method is used to deal with viscous flow with high Reynolds number, the grids near the wall need to be very fine, which results in a large amount of meshes and computation. It limits the application of the method in complex geometric viscous flow problems and its promotion to three-dimensional flows. For this reason, in order to reduce the computational grid demand, especially at the boundary of the object, some scholars [10-13] have studied the application of Cartesian grid method in turbulent viscous flow. An effective idea is to define turbulent wall boundary conditions by using the wall function model derived from the boundary layer approximation theory, so as to reduce the dependence of numerical methods on the scale of the wall mesh, so as to reduce the number of computational meshes in the boundary layer. The wall function method has been verified that it can significantly reduce the dependence of numerical results on grid scale. Usually, the height of the first layer mesh near the wall can be relaxed within the range of $30<y+<200$ based on the use of wall function, which reduces the quantity of grids and enhances the computation efficiency dramatically.

At present, the numerical simulation of viscous flow based on adaptive Cartesian grid has not yet been applied in engineering, and there is a need for further development. The purpose of this paper is to develop a numerical method to simulate two-dimensional high Reynolds number viscous flow automatically, efficiently and accurately. In this paper, an adaptive Cartesian mesh generation technique based on Quadtree data structure is developed. The adaptive process is based on the geometric features of the object surface and the flow field characteristics. It can guarantee the fidelity of geometric shape information and the detailed simulation of shock, shear layer and vortices in the flow field. Aiming at the possible cusps and thin bodies in complex shapes, a Cartesian grid-oriented multi-valued grid processing program is constructed to ensure the accuracy and stability of the simulation near these structures. For boundary treatment, the boundary condition of viscous surface is reconstructed by the immersed boundary method to avoid dealing with complex cut cells and combining virtual mirror symmetry technology. On the basis of this method, a wall function method is introduced into the Cartesian grid framework to reduce the requirement of numerical results for the size of grids in the boundary layer. Based on the above work, a wall boundary treatment method for high Reynolds number viscous flow under adaptive Cartesian mesh is established. After adapting the grid, for the transition region of coarse and fine grids, the flow field value of the computational template points needs special treatment, that is, the hang-grid problem. On this basis, a two-dimensional viscous flow numerical solver based on Cartesian grid is constructed by using appropriate spatial and temporal discrete schemes. In this paper, several typical numerical cases of viscous flow with high Reynolds number is simulated to validate the methodology and numerical solver.

2. Adaptive Cartesian grid generation

2.1 Octree data structure

In the Quadtree data structure, the parent grid cell is refined to four sub-grid cells, and the parent cell and the sub-cell are connected by pointers. This data structure has a small storage capacity and is convenient and efficient for adaptive refinement and coarsening. For example, when the grid is coarsened, only four sub-pointers need to be empty and set to pointless. When the grid is refined, only the sub-pointers need to be allocated memory separately and pointed to sub-grids. The allocation of information storage in grid cells needs to consider both memory occupancy and computational complexity. Generally speaking, the storage content includes three parts, namely, the location information of the grid, the data structure information and the flow field information.

2.2 Neighbor finding

In the Cartesian grid methodology developed in this paper, the grid cells in the Octree data structure do not pre-store the information of neighbor cells, which requires the design of corresponding algorithms to obtain, that is, neighbor finding algorithm. Whether it is reasonable or not can greatly affect the computational efficiency, and moreover, the process of neighbor finding can check the balance and rationality of grid structure. The recursive process is the core part of the neighbor finding algorithm, which queries the neighbor cell of the parent cell and determines the sub-cell of the neighbor cell. This requires algorithm design according to the characteristics of Cartesian grid and Octree data structure. In Figure 1, the process of finding right neighbor cells in different situations is shown, and the finding algorithm of neighbor cells in other three directions is similar. Four sub-cells are labeled i1, i2, i3 and i4 according to their positions, and the four sub-cells of i2 are labeled i21, i22, i23, i24, and so on.

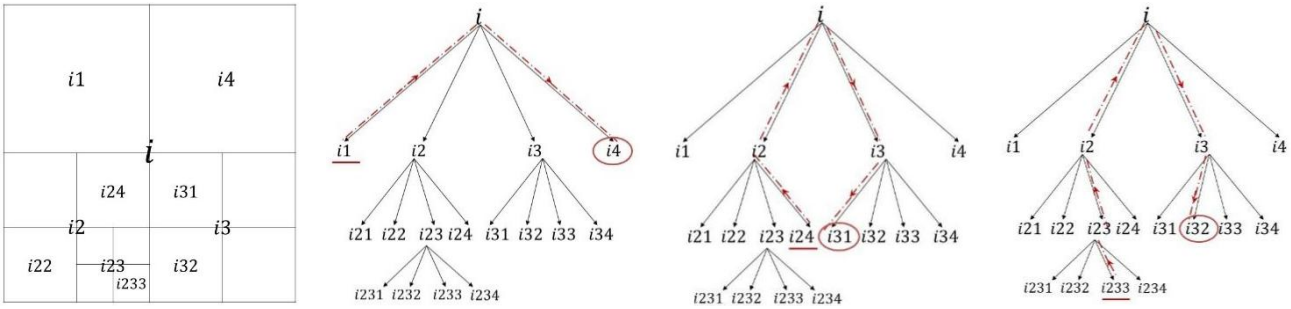

Figure 1 – Neighbor query diagram for grid of different levels

2.3 Grid type determination

Because the immersed boundary method [15-19] uses grids inside the object surface, it is an important work to determine the type of grids. Accurate determination of grid type is the precondition of Cartesian mesh adaptation and subsequent flow field calculation. There are two main methods to classify Cartesian grid cells. One is to divide them into external grid cells, intersecting grid cells and internal grid cells according to the position and intersecting relationship between grid cells and objects. The other is to classify the flow field grid cell outside the object and the ghost cell inside the object according to the position of the grid center point, which are both used in this paper. The de-termination of the type of grid cells is based on the determination of grid point type, and the location of the four vertices of the grid cell needs to be determined respectively.

Based on the ray-casting approach, this paper determines the relationship between grids and objects, and improves the approach by introducing multiple rays to ensure the accuracy of the type determination of grids. In the ray-casting approach, any ray intersects the object surface through a target grid point, and the position relationship between the grid point and the object is determined by the number of intersections. That is, if the number of intersections is even, the grid point is outside the object, and if the number of intersections is odd, the grid point is inside the object, as shown in Figure 2. When using the ray-casting method, we should pay attention to the arbitrariness of ray direction and avoid the misleading of unreasonable special ray to the determination of cell type, as shown in 3. This requirement can be met by the multiple rays method presented in this paper.

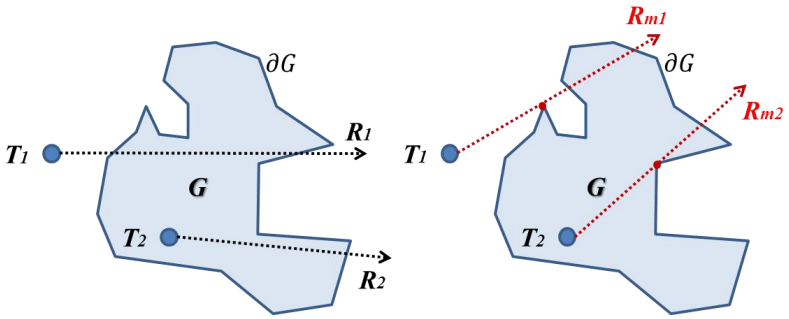

Figure 2 – Ray-Casting Approach.

2.4 Grid adaption

The grid adaptation can be divided into geometric feature adaptation and flow field feature adaptation. Among them, the geometric feature adaptation is based on the geometric characteristics of the object to carry out adaptive refinement, which requires that the shape and structure characteristics of the model can be accurately depicted. It is mainly carried out in two aspects. Firstly, based on the geometric shape of the object, cells intersecting the object surface is refined for a certain number of times. Then, based on the surface curvature of the object, the cells where the surface curvature of the object changes greatly is further refined. In addition, the cells adjacent to the intersecting cells need to be refined a certain number of times to ensure that the grid transition is uniform.

Then, in the process of flow field calculation, it is necessary to adapt to the characteristics of the flow field solution. In order to capture the shock wave and shear layer in the flow field better, the divergence and curl of velocity are combined as the criterion to carry out the flow field solution adaption [14]. The divergence of velocity is mainly used to capture shock wave, and the curl of velocity is mainly used to capture the shear layer. The formulas of the velocity divergence D_{cell} and the curl R_{cell} of the *cell* are as follows:

$$D_{cell} = |\nabla \bullet U| l_{cell}^{\frac{a+1}{a}}, \; R_{cell} = |\nabla \times U| l_{cell}^{\frac{a+1}{a}} \tag{1}$$

In the formula, *l* is the *cell*'s edge length and *a* is a given value. In the two-dimensional case, *a* = 2 .and in the three-dimensional case, *a* = 3.

In the adaptive process of flow field solution, it is necessary to calculate the divergence and curl of velocity for each cell, so that the total number of grid cells in the computational domain is recorded as *N*. After the D_{cell} and R_{cell} values of *N* cells are obtained, the standard deviation S_D of velocity divergence and the standard deviation S_R of velocity curl can be obtained by the following formula:

$$S_D = \sqrt{\frac{\sum {D_{cell}}^2}{N}}, \; S_R = \sqrt{\frac{\sum {R_{cell}}^2}{N}} \tag{2}$$

Then the following conditions are used for grid adaption:

1) if $D_{cell} > \delta_1 * S_D$ or $R_{cell} > \delta_2 * S_R$, the cell is to be refined;
2) if $D_{cell} < 0.1 * \alpha_1 * S_D$ and $R_{cell} < 0.1 * \alpha_2 * S_R$, the cell is to be coarsened;

For the selection of coefficients δ_1, δ_2, α_1, and α_2, we should consider the flow field characteristics [4], because the dominant flow phenomena in the flow field may be different under different conditions:

1) if there is no obvious dominant flow characteristics in the flow field, the above coefficients can be taken as $\delta_1 = \delta_2 = \alpha_1 = \alpha_2 = 1.0$;
2) if the shear layer plays a dominant role in the flow field, the corresponding coefficients can be taken as $\delta_1 = \delta_2 = 2.0, \alpha_1 = \alpha_2 = 0.5$;
3) if the shock wave plays a dominant role, it can be taken as $\delta_1 = \delta_2 = 0.5, \alpha_1 = \alpha_2 = 2.0$.

These coefficients may not be the optimum values, and they need to be adjusted according to the characteristics of the flow field in order to make the adaptive mesh distribution more reasonable.

2.5 Virtual layer technology

For adaptive Cartesian grid, the ratio of the size of coarse grids to fine grids in adjacent layers is constant to 2, even in the boundary layer. The large scale variation of grid size will affect the accuracy and stability of near-wall flow simulation. In order to solve the above problems, this paper introduces the virtual layer technology [14] to optimize the boundary layer mesh, referring to the advantages of body-fitted structured mesh in capturing boundary layer flow characteristics, as shown in Figure 3. Firstly, a series of points N_1, N_2 and N_3 are mapped in the boundary layer along the normal direction of the wall according to a certain rule. The initial virtual layer is generated from the first layer data points, and then the ratio of the virtual layer to the normal distance of the wall is set as follows:

$$1 < \frac{\delta_{n+1}}{\delta_n} < k, (n = 1,2,3, \ldots), \delta_n = |N_{n-1}N_n| \tag{3}$$

Using the distribution characteristics of the body-fitted grid in the boundary layer for reference, the above-mentioned ratio can be set up to obtain a number of virtual surfaces with uniformly varying distances in the boundary layer, whose distances are similar to those of the body-fitted grid. The number and level of refinement of Cartesian grid cells are determined by combining these virtual layers.

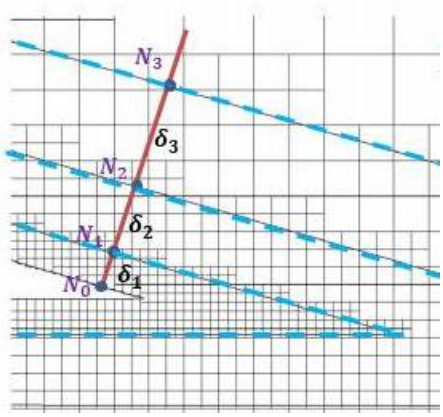

Figure 3 – The virtual layer method.

2.6 Mesh smoothing

In the process of Cartesian mesh refinement and coarsening, the meshes in some areas may be unreasonable, which will generally lead to problems in mesh structure and subsequent flow field calculation. There are many specific types of these unreasonable features. The Cartesian grid method developed in this paper may encounter the following situations:

1) the difference between adjacent grid cells in the hierarchy of the Octree data structure is greater than 1, as shown in Figure 4(a);
2) there are sub-cells in the neighboring cells on both sides of the leaf cell, as shown in Figure 4(b);
3) the cusps are located in the larger grid of leaf cells, and the description of cusp structure is not clear, as shown in Figure 4(c);
4) when there are minimal gaps or inner corners, the boundary between the two sections is in the same grid cell, as shown in Figure 4(d).

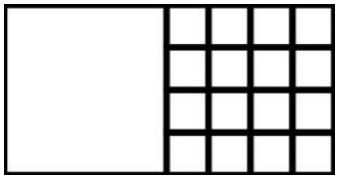

（a）The level difference between adjacent cells is greater than 1

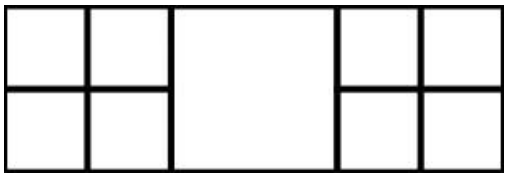

（b）Hole grid

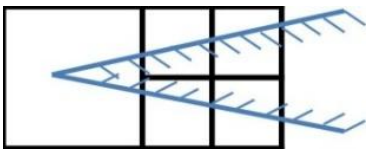

（c）The grid cell at the cusp is too large

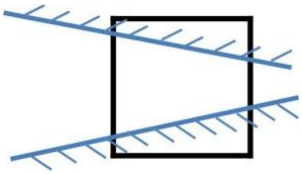

（d）The two boundaries are in the same grid

Fig. 4 – Unreasonable characteristics of Cartesian grid

Generally speaking, these unreasonable features are mainly unreasonable or complicated data structure, inaccurate description of object shape or inadequate feature capture, and will affect the stability, convergence and accuracy of flow field calculation. Therefore, the existence of unreasonable grid cells can not be ignored. The process of eliminating them and optimizing mesh is called mesh smoothing. The mesh smoothing process is carried out after the grid adaption, and needs to be processed repeatedly until all the unreasonable features are eliminated, so that the distribution of the mesh can be improved as much as possible to improve the accuracy of the shape description, while meeting the requirements of the balance and efficiency of the Octree data structure. It lays the foundation for the flow field solution adaption.

3. Boundary treatment methodology

3.1 Immersed boundary approach

For Cartesian grid methodology, when the immersed boundary approach is used to deal with the object surface boundary, the grid cell inside the object, namely the ghost cell, is used. In this paper, the flow field information of these cells is obtained by ghost cell method, Figure 5 is taken as an example. In order to obtain the flow field value of ghost cell *A*, the image point M_A of A in the flow field should be determined first, and the flow field value of M_A can be obtained by interpolation of adjacent cells. Then, according to the boundary conditions of the object surface, i.e. the non-penetration, non-slip of the wall velocity, the relationship between the flow field values of ghost cell *A* and mirror point M_A is determined, and the flow field information at virtual point *A* is obtained. For the mirror point M_A of ghost cell *A*, the interpolation formula of flow field information is as follows:

$$q_{M_A} = \frac{e^{-|r_1|}q_C + e^{-|r_2|}q_D + e^{-|r_3|}q_E + e^{-|r_4|}q_F}{e^{-|r_1|} + e^{-|r_2|} + e^{-|r_3|} + e^{-|r_4|}} \tag{4}$$

In the formula, r_1, r_2, r_3, r_4 are the distances from M_A to its four adjacent grid points *C, D, E* and *F* respectively.

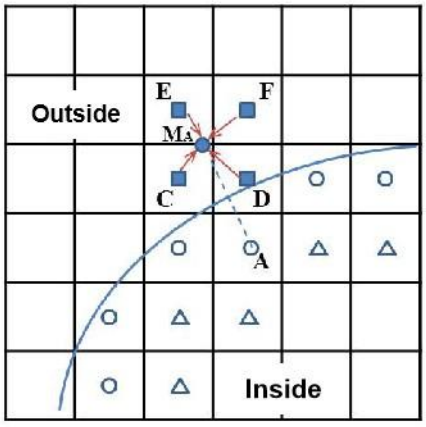

Figure 5 – The Ghost Cell method.

In order to simulate the boundary conditions more accurately, the Ghost Body-Cell Method (GBCM) proposed by Dadone and Grossman et al. [19] is used in this paper. This method is extended from the Curvature-Correction Symmetry Technique (CCST) first proposed by Dadone et al. [17-19], which is suitable for body-fitted grids. The flow field values of ghost cells are obtained by the fictitious eddy field near the object surface, and the entropy and total enthalpy of the eddy field are symmetrically distributed in the normal direction. Dadone et al. show that the GBCM method has

more advantages than the traditional surface boundary treatment method in ensuring the increase of entropy and the decrease of total enthalpy, and is conducive to the stability and convergence of the calculation.

In view of the characteristic structure of boundary layer in viscous flow with high Reynolds number, when using GBCM method to reconstruct wall boundary conditions, the reference points of ghost cells are adjusted geometrically, which makes it more advantageous to characterize the internal characteristics of boundary layer. Moreover, the distance between reference point and object surface can be aligned by position adjustment, which has some characteristics of structured body-fitted grid and improves the stability of interpolation, as shown in Figure 6. Forrer and Beger et al. [20] showed that this position adjustment can improve the stability of calculation, and does not reduce the accuracy of boundary processing. The disadvantage is that the local conservation of mass and momentum is difficult to guarantee. Based on GBCM and the idea of position adjustment, the flow field values of ghost cell A and mirror point B in this paper satisfy the following relationships:

$$\begin{cases} p_A = p_B - \rho_B \left(\dfrac{\widetilde{u}_B{}^2}{R_B}\right) \cdot n_{AB} \\ n_{AB} = \delta_l + \delta_g \\ \rho_A = \rho_B \left(\dfrac{p_A}{p_B}\right)^{\frac{1}{\gamma}} \\ \widetilde{u}_A{}^2 = \widetilde{u}_B{}^2 + \dfrac{2\gamma}{\gamma - 1}\left(\dfrac{p_B}{\rho_B} - \dfrac{p_A}{\rho_A}\right) \\ \tilde{v}_A = -\tilde{v}_B \end{cases} \tag{5}$$

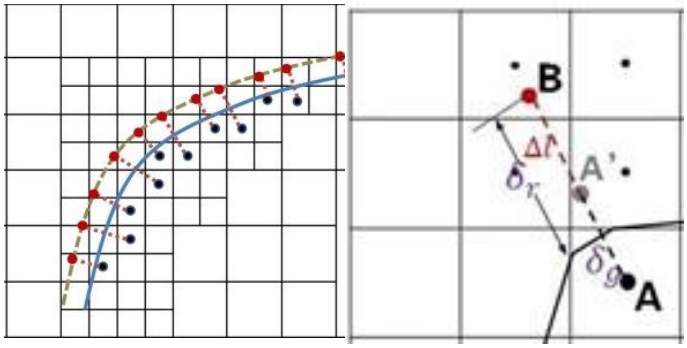

Figure 6 – Near wall grid point correction.

3.2 Wall function method

Wall Function Method (WFM) is an empirical model derived from boundary layer theory, which needs to satisfy a series of simplified assumptions [21,22]. In this paper, the wall function model proposed by Spalding [21] is used and applied in Cartesian grid. The model is simple and has been verified by many scholars. It has high reliability. Its definition is as follows:

$$y^+ = u^+ + e^{-kB}[e^{ku^+} - 1 - ku^+ - \frac{(ku^+)^2}{2} - \frac{(ku^+)^3}{6}] \tag{6}$$

y + and *u* + are defined as dimensionless boundary layer thickness and velocity in boundary layer respectively. They are defined as follows:

$$u^+ = v_t / u_\tau, y^+ = \frac{\rho_w u_\tau y}{\mu_w}, u_\tau = \sqrt{\frac{\tau_w}{\rho_w}} \tag{7}$$

According to the basic assumption of wall function and the Crocco-Busemann relationship, the pressure and temperature on the wall can be obtained.

$$P_w = P_{ref}, \quad T_w = T_{ref} + \frac{r}{2}\frac{V_{T,ref}^2}{C_p} \tag{8}$$

According to the basic assumption of wall function, the shear stress near the wall is a constant

distribution, so it can be considered that the shear stress between the reference point and the virtual element should remain unchanged. Combined with Newton's friction stress formula, the corresponding tangential and normal velocity components of ghost cells, as well as the pressure and temperature values, can be obtained as follows:

$$\tau = \mu \frac{\partial v_t}{\partial n} \approx \mu \frac{V_T - V_w}{\Delta n}$$

$$\boldsymbol{V}_{Tg} \approx \boldsymbol{V}_{Tref} - (\frac{\delta_r + \delta_g}{\mu_{ref} + \mu_{tref}})\boldsymbol{t}, \boldsymbol{V}_{Ng} = -\frac{\delta_g}{\delta_r}\boldsymbol{V}_{Nref} \tag{9}$$

$$P_g = P_{ref}, T_g = T_{ref} + \frac{r}{2}\frac{\boldsymbol{V}_{Tref}^{\ 2} - \boldsymbol{V}_{Tg}^{\ 2}}{C_p}$$

For turbulence problems, because of the application of turbulence model, it is necessary to determine the turbulence viscous coefficient of ghost cell. For Spalding turbulent wall function, the relationship between turbulent viscous coefficient and laminar viscous coefficient near the wall can be obtained by deriving *y*+ to *u*+:

$$\frac{\mu_\tau}{\mu_l} = ke^{-kB}[e^{-kB} - 1 - ku^+ - \frac{(ku^+)^2}{2}] \tag{10}$$

According to the fact that the total viscous coefficient of the ghost cell is equal to that of the reference point, the turbulent viscous coefficient of the ghost cell can be obtained as follows:

$$\mu_{tg} = \mu_{ref} + \mu_{tref} - \mu_g \tag{11}$$

For different turbulence models, there are other different flow variables. Taking SST turbulence model as an example, the values of turbulence *k* and ω are need to be calculated. The methods of obtaining the values of other turbulence models are similar.

$$k = \frac{\omega \mu t}{\rho}, \omega = \sqrt{\omega_i^{\ 2} + \omega_o^{\ 2}}$$

$$\omega_i = \frac{6\mu_w}{0.075\rho_w y^2}, \omega_o = \frac{\mu t}{\sqrt{C_\mu} ky} \tag{12}$$

4. Viscous flow solver

4.1 Governing equations

The governing equation in this paper is the compressible Reynolds averaged Navier-Stokes (RANS) equation of the ideal state gas. Its conservative form is as follows:

$$\frac{\partial \boldsymbol{U}}{\partial t} + \frac{\partial \boldsymbol{E}}{\partial x} + \frac{\partial \boldsymbol{F}}{\partial y} = \frac{\partial \boldsymbol{E}_\gamma}{\partial x} + \frac{\partial \boldsymbol{F}_\gamma}{\partial y} \tag{13}$$

In the formula, $\boldsymbol{U}$ is a conservative variable, $\boldsymbol{E}$, $\boldsymbol{F}$ are convective terms, $\boldsymbol{E}_\gamma$, $\boldsymbol{F}_\gamma$ are viscous terms. If $\boldsymbol{E}_\gamma$ and $\boldsymbol{F}_\gamma$ are neglected, the above equation will degenerate into Euler equation. The expressions of the above items are as follows:

$$\boldsymbol{U} = \begin{pmatrix} \rho \\ \rho u \\ \rho v \\ E_t \end{pmatrix} \quad \boldsymbol{E} = \begin{pmatrix} \rho u \\ \rho u^2 + p \\ \rho uv \\ (E_t + p)u \end{pmatrix} \quad \boldsymbol{F} = \begin{pmatrix} \rho v \\ \rho uv \\ \rho v^2 + p \\ (E_t + p)v \end{pmatrix}$$

$$\boldsymbol{E}_\gamma = \begin{pmatrix} 0 \\ \tau_{xx} \\ \tau_{xy} \\ u\tau_{xx} + v\tau_{xy} + k\dfrac{\partial T}{\partial x} \end{pmatrix} \quad \boldsymbol{F}_\gamma = \begin{pmatrix} 0 \\ \tau_{yx} \\ \tau_{yy} \\ u\tau_{yx} + v\tau_{yy} + k\dfrac{\partial T}{\partial y} \end{pmatrix} \tag{14}$$

$$E_t = \rho(e + \frac{u^2 + v^2}{2})$$

In the formula above, ρ is density, u is velocity component in X axis, v is velocity component in Y axis, p is pressure, E_t is total energy, e is internal energy. Since the number of unknowns in the system of equations is more than the number of equations, the system of equations is not closed, and the equation of state needs to be supplemented：

$$e = \frac{p}{(\gamma - 1)\rho} = \frac{RT}{\gamma - 1} \tag{15}$$

The $\tau_{ij}(i, j = x, y)$ are viscous stress tensors. The expressions are as follows:

$$\begin{aligned} \tau_{xx} &= -\frac{2}{3}\mu\left(\frac{\partial u}{\partial x} + \frac{\partial v}{\partial y}\right) + 2\mu\frac{\partial u}{\partial x} \\ \tau_{yy} &= -\frac{2}{3}\mu\left(\frac{\partial u}{\partial x} + \frac{\partial v}{\partial y}\right) + 2\mu\frac{\partial v}{\partial y} \\ \tau_{xy} &= \tau_{xy} = \mu\left(\frac{\partial u}{\partial x} + \frac{\partial v}{\partial y}\right) \end{aligned} \tag{16}$$

Among them, μ is a viscous coefficient, which includes laminar viscous μ_L and turbulent viscous coefficient μ_T, namely:

$$\mu = \mu_L + \mu_T \tag{17}$$

The μ_L can be obtained from Sutherland formula:

$$\mu_L = \mu_0(\frac{T}{T_0})^{1.5}\frac{T_0 + C}{T + C} \tag{18}$$

The μ_T can be calculated by the turbulence model. For turbulent viscous flow, the effect of turbulence should be taken into account in the heat transfer coefficient.

$$k = c_p\left(\frac{\mu_L}{Pr} + \frac{\mu_T}{Pr_T}\right) = \frac{\gamma R}{\gamma - 1}\left(\frac{\mu_L}{Pr} + \frac{\mu_T}{Pr_T}\right) \tag{19}$$

In the formula, Pr_T is a turbulent Prandtl constant, and for air, Pr_T=0.9.

4.2 Numerical discretization

The unsteady and multi-scale characteristics of turbulence require high-fidelity numerical simulation methods, which solves RANS equation of high accuracy. Considering the flow characteristics of compressible turbulence, spatial and temporal discrete schemes with both accuracy and robustness are very important for high-precision turbulence simulation in this study. In the aspect of spatial discretization for the RANS equation, we use the higher order Weighted Essential Non-Oscillatory (WENO) scheme [23] in the Cartesian grid framework. Among many high-order schemes, WENO scheme has the advantages of relatively few interpolation template points, high accuracy and good robustness. It is very suitable for solving high Reynolds number compressible turbulence problems.

In terms of temporal advance, this paper adopts explicit method to discretize temporal terms. The explicit method transforms the Partial Differential Equation into Ordinary Differential Equation by discretizing the space derivative terms rather than the time derivative term. This method has the advantages of simple form, wide applicability, short single-step time, easy realization of high-order accuracy and parallel computing, but its shortcoming is that its time step is limited by stability conditions. Considering the above characteristics, this paper adopts Total Variation Decrease (TVD) Runge-Kutta method [24]. Taking its third-order accuracy formula as an example:

$$\frac{d\boldsymbol{Q}}{dt} = R(\boldsymbol{Q}) \tag{20}$$

$$
\begin{cases}
\mathbf{Q}^0 = \mathbf{Q}^n \\
\mathbf{Q}^{(1)} = \mathbf{Q}^{(0)} + \Delta t \cdot \mathbf{R}(\mathbf{Q}^{(0)}) \\
\mathbf{Q}^{(2)} = \frac{3}{4}\mathbf{Q}^{(0)} + \frac{1}{4}\mathbf{Q}^{(1)} + \frac{1}{4}\Delta t \cdot \mathbf{R}(\mathbf{Q}^{(1)}) \\
\mathbf{Q}^{(3)} = \frac{1}{3}\mathbf{Q}^{(0)} + \frac{2}{3}\mathbf{Q}^{(2)} + \frac{2}{3}\Delta t \cdot \mathbf{R}(\mathbf{Q}^{(2)}) \\
\mathbf{Q}^{n+1} = \mathbf{Q}^{(3)}
\end{cases}
$$

The WENO scheme for spatial discretization matching by Runge-Kutta method with high precision has high accuracy and can reduce shock discontinuity as well as oscillation near turbulent boundary layer, so as to construct a high-accuracy and robust numerical solver for high Reynolds number turbulent flow problems.

5. Numerical results

Next, numerical simulations are carried out for typical examples to examine the adaptive Cartesian grid generation technology developed in this paper and the numerical simulation method of high Reynolds number viscous flow in Cartesian mesh.

5.1 Flat plate

The adiabatic flow on a flat plate is a classic example for studying laminar and turbulent viscous flows. In this paper, the wall function model and numerical method for high Reynolds number viscous flow simulation developed in this paper are tested and validated.

Firstly, two-dimensional laminar plate flow is simulated. In this simulation, the Reynolds number based on the plate length is $\mathrm{Re} = 1.0 \times 10^3$. The numerical result is compared with the Blasius solution [25] in Fig. 7. It shows the velocity profile interpolated along the vertical direction at two different axial position, i.e. x = 0.75, 0.80. It can be seen that the results obtained by the numerical solver constructed in this paper are in good agreement with the reference solutions.

On the basis of the above work, the wall function method developed in this paper is applied to study the two-dimensional turbulent plate flow. Referring to literature [26], the parameters are set, in which the inflow Mach number is Ma = 0.2, and the Reynolds number is $\mathrm{Re} = 1.0927 \times 10^7$. In Fig. 8, the surface friction coefficient calculated based on different grid scale is compared with the experimental value [27] and result obtained by the Power law.

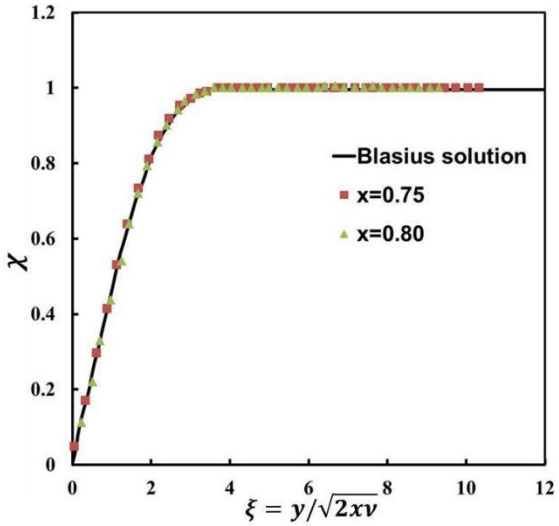

Figure 7 – The velocity profile compared with Blasius solution

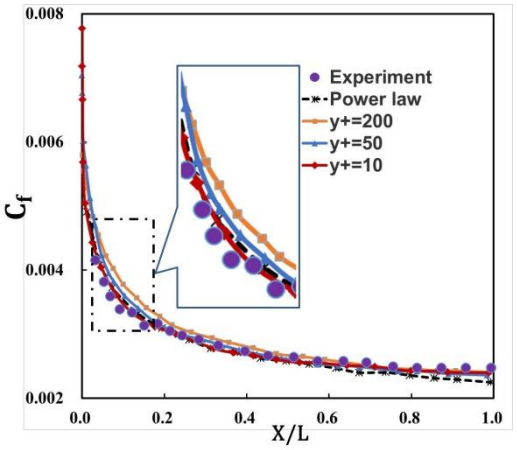

Figure 8 – Computed Cf over turbulent flat plate

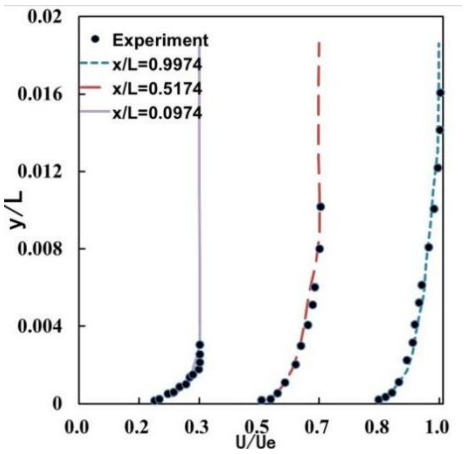

Figure 9 – Mean velocity profiles on turbulent flat plate

In Fig. 8, it can be seen that the numerical results in this paper still show high accuracy when y+ is large by using the wall function method, the dependence of the numerical results on the grid scale is greatly reduced. As y+ decreases, the deviation between the calculated friction results and the reference results decreases, which is caused by insufficient mesh refinement. In the trailing edge region of the plate, even the results based on coarse mesh are in good agreement with the experimental and reference values.

Fig. 9 shows the comparison between the calculated average velocity profiles at different positions and the experimental measurements. It can be seen that the calculated average velocity profiles and boundary layer thickness are in good agreement with the experimental measurements. At the three locations in the graph, the predicted boundary layer thickness is slightly larger than the experimental value, which is due to the insufficient mesh refinement and the inadequate ability to capture the velocity gradient.

5.2 NACA0012 airfoil

Aiming at the turbulent flow around NACA0012 airfoil, the method and technology in this paper are further verified. The calculation condition parameters refer to AGARD experimental report [27] and are set as follows: Mach number Ma = 0.3, angle of attack $\alpha = 3.59°$ and Reynolds number $\mathrm{Re} = 1.86 \times 10^6$ based on airfoil chord length.

In this paper, based on the adaptive Cartesian grid ghost cell method, the comparative analysis of the calculation results before and after the introduction of the wall function method is carried out. Firstly, the effectiveness of the wall function method under the Cartesian grid framework is evaluated under different grid densification and scale.

It can be seen from Fig. 11 that the experimental results are in good agreement with the three kinds of refinement times and grid scale, which proves that the wall function method developed in this paper is also suitable for the adaptive Cartesian grid. Generally speaking, the results of the three methods are similar to each other. This is because in the wall function method, a unified simplified analytical function is used. In the relaxed limit of the wall mesh size, the grid point values are not obtained by the wall mesh through the numerical discrete scheme, but by the approximate analytical function. Therefore, the larger mesh can still maintain the accuracy of the solution. Of course, improving the resolution of the grid can improve the accuracy of the analytical function calculation results. Therefore, the accuracy of the grid refinement 10 times is slightly improved than that of the grid refinement 8 times and 9 times, which is mainly reflected in the leading edge and trailing edge positions of the airfoil which are more sensitive to the grid scale.

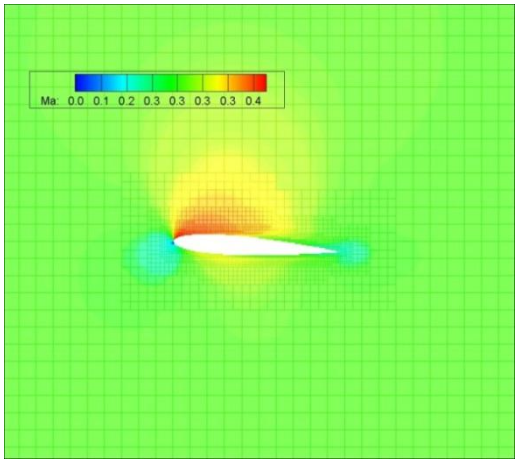

Figure10 – Mach number contour and grid of flow field.

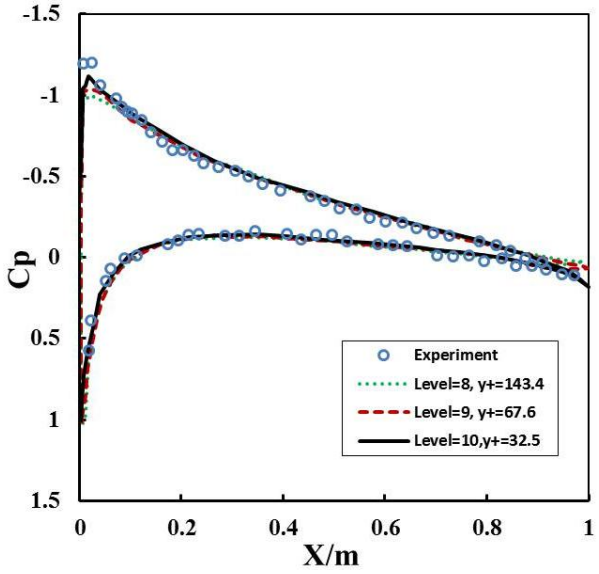

Figure11 – Comparison of airfoil surface pressure coefficients at different grid scales.

6. Conclusions

In this paper, the adaptive Cartesian grid methodology for two-dimensional viscous flow is developed. The adaptive grid technique and the surface boundary treatment based on immersed boundary approach are systematically constructed. Aiming at the difficulty of simulating high Reynolds number viscous flow with Cartesian grid method, the boundary layer mesh optimization technology based on virtual layer technology and the wall function method to relax the size limitation of near-wall grids are developed. The numerical solver for high Reynolds number viscous flow is constructed. On this basis, the assessment and validation of techniques and methods developed are completed through the simulation of typical examples. By introducing the wall function model, on the premise of guaranteeing the accuracy of simulation, the requirement of near-wall grids size can be reduced, and it can get better simulation accuracy on the coarse grid.

7. Acknowledgements

This work was supported by National Numerical Windtunnel project and State Key Laboratory of Aerodynamics Research Fund.

8. Copyright Statement

References

[1] MAVRIPLIS D J. An advancing front Delaunay triangulation algorithm designed for robustness[J]. Journal of Computational Physics, 1995, 117(1): 90-101.

[2] ITO Y, NAKAHASHI K. Unstructured hybrid grid generation based on isotropic tetrahedral grids: AIAA-2002-0861 [R]. Reston, VA: AIAA, 2002.

[3] KALLINDERIS Y, WARD S. Prismatic grid generation with an efficient algebraic method for aircraft configuration: AIAA-1992-2721. [R]. Reston, VA: AIAA, 1992.

[4] DE ZEEUW D L. A quadtree-based adaptively-refined Cartesian-grid algorithm for solution of the Euler equations[D]. University of Michigan, 1993.

[5] MURAT B. Quadtree-based adaptively-refined Cartesian-grid algorithm for solution of the Euler equations[D]. University of Michigan, 2005.

[6] ROBERT R A, VLADIMIR I K. Direct simulation Monte Carlo with octree Cartesian mesh[J]. AIAA Journal. 2012, 20(2): 25-28.

[7] FUJIMOTO K, FUJII K, WANG Z J. Improvements in the reliability and efficiency of body-fitted Cartesian grid method: AIAA-2009-1173[R]. Reston, VA: AIAA, 2009.

[8] UDAYKUMAR H S. Multiphase dynamics in arbitrary geometries on fixed Cartesian grids[J]. Journal of Computational Physics, 1997, 137: 366-405.

[9] UDAYKUMAR H S. A sharp interface Cartesian grid method for simulating flow with complex moving boundaries[J]. Journal of Computational Physics, 2001, 174: 345-380.

[10]MARSHALL D D. Extending the functionalities of Cartesian grid solvers: viscous effects modeling and MPI parallelization[D]. Georgia Institute of Technology, 2002.

[11]FORRER H, JELTSCH R. A higher order boundary treatment for Cartesian-grid method[J]. Journal of Computational Physics, 1998, 140: 259-277.

[12]Jae-Doo L, Ruffin S M. Development of a turbulent wall-function based viscous Cartesian-grid methodology: AIAA-2007-1326[R]. Reston, VA: AIAA, 2007.

[13][JAE-DOO L. Development of an efficient viscous approach in a Cartesian grid framework and application to rotor-fuselage in-teraction[D]. Georgia Institute of Technology, 2006.

[14]Ya'eer Kidron, Yair Mor-Yossef. Turbulent flow predictions using a Cartesian flow solver [C]. 19th AIAA Computational Fluid Dynamics, San Antonio, Texas. AIAA Paper, 2009-3881.

[15]Peskin C S. Flow patterns around heart valves: a numerical method [J]. Journal of Computational Physics, 1972, 2: 252–271.

[16]Mohd Y. Combined immersed boundary/B-Spline methods for simulations of flow in complex geometries [C]. CTR Annual Research Briefs, Center for Turbulence Research, NASA Ames/Stanford Univ, 1997, 317-27.

[17]Dadone A, Grossman B. Ghost-cell method for inviscid two-dimensional flows on Cartesian grids [J]. AIAA Journal, 2004, 42: 2499-2507.

[18]Dadone A, Grossman B. An immersed body methodology for inviscid flows on Cartesian grids [C]. AIAA Paper, 2002-2328.

[19]Dadone A, Grossman B. Further developments in the three-dimensional Cartesian grid ghost cell method [C]. AIAA Paper, 2006-1085.

[20]Forrer H, Jeltsch R. A higher-order boundary treatment for Cartesian-grid methods [J]. Journal of Computational Physics, 1998, 140: 259-277.

[21]Spalding D B. A single formula for the law of the wall [J]. Journal of Applied Mechanics, 1961, 28(3): 455-458.

[22]Nichols R H, Nelson C C. Wall function boundary conditions including heat transfer and compressibility for transport turbulence models [C]. AIAA Paper, 2004-582.

[23]Pirozzoli S. Conservative hybrid compact-WENO schemes for shock-turbulence interaction[J]. J Comp Phys, 2002, 178: 81-117.

[24]Gusiafsson B, Sandstrom A. Incompletely parabolic problems in fluid dynamics [J]. Journal of Applied Mathematics, 1978, 35: 343-357.

[25]Blasius H. Grenzschichten in flüssigkeiten mit kleiner Reibung[J]. Z. Math. Phys. 1908 (56) :1–37.

[26]Wieghardt K, Tillmann W. On the turbulent friction layer for rising pressure. NACA TM 1314, 1995.

[27]Thibert J J, Grandjacques M, Ohman L H. Experimental Data Base for Computer Program Assessment. AGARD Advisory Report No. 138, 1979.

[28]Tang Zhigong, Chen Hao, Bi Lin, et al. Simulation of supersonic viscous flow based on adaptive Cartesian grid[J].Acta Aeronautica et Astronautica Sinica, 2018, 39(5): 121697.